Nutrient limitation predisposes a cultivate of *Burkholderia contaminans* from the ISS water processor assembly to biofilm formation under simulated microgravity.

Angie Diaz[1], Anirudha R. Dixit[1], Christina LM. Khodadad[1], Mary E. Hummerick[1], Yo-Ann Justiano-Velez[2], Wenyan Li[1] and Aubrie O'Rourke[3*]

[*] Corresponding author: aubrie.e.orourke@nasa.gov

Affiliations:

[1] Amentum Services, Inc, LASSO, NASA Kennedy Space Center, Merritt Island, FL, USA
[2] Space Systems Department, NASA Marshall Space Flight Center, Huntsville, AL, USA
[3] Exploration Research and Technology, NASA Kennedy Space Center, Merritt Island, FL, USA

Abstract

The International Space Station (ISS) Water Processor Assembly (WPA) experiences intermittent dormancy between water recycling events thus promoting biofilm formation within the system. In this work we aimed to gain a deeper understanding of the impact of nutrient limitation on bacterial growth and biofilm formation under microgravity in support of biofilm mitigation efforts in exploration water recovery systems. A representative species of bacteria that is commonly cultured from the ISS WPA was cultured in an WPA influent water ersatz formulation tailored for microbiology studies. *Burkholderia contaminans* was cultured under a simulated microgravity (SμG) treatment in a vertically rotating high-aspect rotating vessel (HARV), with a rotating control (R) in the horizontal plane at the determined optimal rpm of 15 along with a stationary (S) control. At different time points, the bacterial culture and ersatz were harvested for bacterial counts, transcriptomic and nutrient content analyses. Under the test conditions, the culture under SμG treatment consumed the essential nutrients faster than the R and S control cultures in the early stage of growth, thus approaching a nutrient limited growth condition earlier than the controls. The rapid uptake and subsequent depletion of essential nutrients was further illustrated in the transcriptomic response of the SμG culture when compared to the transcriptomic response of the R and S control conditions. The observed starvation response may serve as one element to explain a moderate enhancement of biofilm formation in the SμG treatment. One implication of this investigation is that biofilm mitigation in the ISS environment could be supported by ensuring a steady flow of water as a vehicle for essential nutrients within the WPA to avoid complete consumption which occurs in times of no flow lending to undesired biofilm formation.

Background

This study aimed to address the biofilm formation under microgravity knowledge gap with a focus on the microbe, *Burkholderia contaminans*, that is commonly isolated from biofilms of the International Space Station (ISS) Water Processor Assembly (WPA). Biofilms consist of microbial communities sheltered in a self-produced extracellular matrix that greatly improves the ability of

the bacterial cells to survive and thrive under environmental stresses (Zea et al. 2018). Biofilm control is an important and challenging aspect of life on Earth and in space. Microbial contamination onboard the ISS continues to pose mission risks to both crew health and hardware reliability (Diaz et al. 2019). Formation of biofilms, harboring *B. contaminans* among other species, in the water recovery system can cause biofouling that can lead to blockage and system failure during long term missions. The ISS WPA produces potable water from a combination of humidity condensate and urine distillate produced from the Urine Processor Assembly. In late 2009, the inlet solenoid valve to the Mostly Liquid Separator (MLS) of the assembly was obstructed with a biofilm, which led to multiple operation modifications, including tank cycling, regular flushing with iodinated water, as well as the installation of a 250-micron filter before the solenoid valve, which requires annual replacement (Velez Justiniano et al. 2021).

The effect of microgravity on bacterial growth and biofilm formation is a knowledge gap for biofilm management in space. However, it is known that under ambient gravity conditions, density-driven convection allows for the mixing of a bacterial culture, which speeds up the mass transfer rates of nutrients to cells and waste products away from cells. Conversely, under microgravity, objects of different densities travel at the same velocity, motionless relative to each other, thus no density-driven convection or cell settlement occurs. In microgravity, if there is no forced mixing, mass transfer occurs through diffusion alone (Benoit and Klaus 2007). The lack of sedimentation in the spaceflight environment is thought be of benefit to non-motile cells as they can more readily access by-products required for growth. This is evident by an observed early emergence from lag phase and a longer exponential growth phase for non-motile cultures relative to terrestrial control cultures (Zea et al. 2016). Single cell gravitational sensing theoretical assessments predict that bacteria may be too small to be directly affected by weightlessness and that indirect effects shape the response (Albrecht-Buehler 1991). These indirect effects are induced by microgravity-mediated changes such as altered mechanical forces of the surrounding liquid, as well as the abovementioned nutrients and wastes surrounding the cell. This differs from the direct effects of weightlessness that are experienced due to a change in g-force (Klaus et al. 2004). The picture is not yet complete enough to understand the effect of weightlessness on multicellular biofilms, however, we can deduce the effect of nutrient availability on biofilm formation under microgravity conditions through experimentation.

In a Space Shuttle investigation (Kim et al. 2013), a greater final cell density was observed for the bacteria, *Pseudomonas aeruginosa* in true spaceflight as compared to gravity controls, when cultured in a modified artificial urine media, consisting of a low concentration of phosphate combined with decreased oxygen availability, It was determined that cell motility did not influence cell density outcomes, but if phosphate or oxygen was increased, the difference in final cell density was no longer observed. It was similarly observed in *Salmonella* that effects such as increased virulence and acid tolerance in actual spaceflight as well as low shear modeled microgravity (LSMMG) cultures could be minimized by increasing phosphate concentration or by supplementing media with inorganic ions (Rosenzweig et al. 2010). Furthermore, a cultivate of *Burkholderia cepacia* isolated from the Space Shuttle water system was grown on Shuttle in an experiment using sterile water (a low nutrient condition) and tryptic soy broth (TSB; a high

nutrient condition) for six days exposed to stainless-steel coupons. Biofilm formation on the returned coupons was assessed and revealed that the samples grown in the low nutrient condition exhibited a biofilm plate count that was five times greater than that of the terrestrial control whereas, the high nutrient culture from spaceflight had one fourth the amount of biofilm formation compared to the terrestrial control (Pyle et al. 1999). This further suggests that nutrient limitation can lead to increased biofilm formation under microgravity conditions. Such This metabolic starvation can be observed in the transcriptomic response of the culture where the impact of microgravity on broader bacterial metabolism presents a signature of starvation as cells alter their metabolic strategies to harvest available energy sources which are either internally generated or novel external sources of carbon (Sharma and Curtis 2022).

High Aspect Ratio Vessels (HARVs) have been used in combination with Rotating Wall Vessel (RWV) bioreactors to simulate the low fluid-shear levels in LSMMG, which has been validated through mathematical calculation (Nauman et al. 2007) and mass transfer studies (Crabbé et al. 2010; A. Diaz et al. 2022). Microarray analysis of *P. aeruginosa* PAO1 grown in the low shear modelled microgravity (LSMMG) environment of the RWV for 24 hours, as compared with the horizontally rotating ambient gravity control, revealed a role for the alternative sigma factor AlgU (RpoE-like) in regulating transcripts encoding stress-related proteins (Crabbe 2010). Additionally, genes encoding chaperones, citric acid cycle enzymes, ATP synthases, cytochromes and ribosomal subunits were found to be up regulated both in the simulated and in the true spaceflight setting. Due to this prior proof of concept, we have used the HARV plus RWV set up to simulate microgravity for a culture of *B. contaminans* and further implemented both a horizontally rotating gravity control and horizontal static gravity control to evaluate how each culture differentially consumes the nutrients from a defined ersatz formula overtime and to identify a robust cellular response to nutrient limitation which may set apart the simulated microgravity culture.

Materials and Methods

Cell culture

A B. contaminans ISS isolate was received from Johnson Space Center as a trypticase soy agar (TSA) plate culture and its identification confirmed at Kennedy Space Center (KSC) by both 16S rRNA confirmation and whole genome sequencing. A frozen stock was prepared by streaking a single colony from a TSA plate and inoculating into a 250 mL Erlenmeyer flask containing 20 mL TSB. The culture was incubated at 27 °C with shaking at 220 rpm. At OD600=1 the culture was harvested and mixed to a final concentration of 15 % glycerol and 150 µl aliquots were frozen in sterile microtubes at -80 °C. For each of the three biological replicate experiments, a frozen sample was pulled from the freezer, and with a sterile loop, plated on TSA to grow individual colonies over 24 hours in the 27 °C incubator. A sterile loop was used to select an individual colony to inoculate into a 125 ml Erlenmeyer flask containing 20 ml TSB then incubated at 27 °C with shaking at 220rpm, for 18 hours before HARV inoculation. 1 mL of culture was placed in a microcentrifuge tube. and centrifuged at 5000 rpm for 5 min, and the pellet was resuspended in 1 mL of 0.9% saline vortexed, and then centrifuged again. The process was repeated for a total of three washes and resuspended in ersatz, after which absorbance was taken at 600nm on a spectrophotometer (Gensys 20, Thermo Scientific, CA, US).

Preparation of inoculum

The target absorbance in ersatz was an optical density at 600nm (OD600) of 0.2 yielding approximately 1 x 10^8cells. Once adjusted to near 0.2 in ersatz, 198 µL was taken and inoculated into 1980mL of ersatz for a final cell count of approximately 1 x 10^4. A sample was taken immediately after inoculating ersatz, diluted, and plated onto TSA to confirm the initial (T=0) cell count.

Culture Media: Ersatz

The media used in the HARVs in this study was the current version of the WPA input ersatz; the composition information can be found in Supplemental Table 1. This formula was developed based on available historical composition data of the International Space Station (ISS) WPA tank influent streams (Velez Justiniano et al. 2021).

Inoculation of HARVs on RWV

Three sets of HARV tests were carried out. Each set of HARV tests covered the three rotation conditions: simulated microgravity SµG (vertical rotating), rotating control R (horizontal rotating), and static control S (horizontal non-rotating). Samples were collected at four time points for each rotation condition: T1(24 hours), T2 (28 hours), T3 (32 hours), and T4 (50 hours). The HARVs were filled in the order of the time points, from T1 to T4, in four rounds. A "round" is a set of HARVs prepared within the same timespan (~ 10 minutes) for one timepoint with one HARV for each rotation condition of SµG, R and S. For each round, a sterile 500 mL beaker was filled with ~200 mL of inoculated ersatz. At T0, a sample of 600 µL was pulled from the beaker and an absorbance reading and plating was completed to determine CFU/mL. A sterile 50 mL syringe was used to sample 60 mL from the ersatz culture then attached to one of the HARV ports and the culture injected avoiding introduction of air bubbles. If air bubbles were present, they were removed by gentle tapping on the HARV unit and removal through one of the ports using the syringe. Once all the HARVs were prepared each was placed on the corresponding RWVs set at different orientations and the optimal rotating condition of 15 revolutions per minute (A. Diaz et al. 2022) was set. At the end of the process 30 mL of unused ersatz culture solution was vacuum filtered through a 0.2 µm membrane for water analysis. The remaining 1 liter of T0 ersatz culture was processed for transcriptomic sequencing.

Sample collection

At each time point T1 (24 h), T2 (28 h), T3 (32 h), and T4 (50 h) after T0, the HARVs (SuG, R, and S) were removed from the RWV without disturbing the HARVs for other time points. The cultures were then processed for chemistry, microbial and molecular analyses. For each HARV the solution was drained into a pre-labeled, sterile 50 mL tube and subdivided into700 µL of culture for absorbance measurement and CFU/mL plating, and 20 mL of culture was filtered using a 0.22 µm syringe filter for chemical analysis. A second 20 mL aliquot of unfiltered culture was concentrated for molecular transcriptomic analysis using the CP SELECT™ benchtop concentrator with 0.2 µm PS hollow fiber concentrating pipette tips (InnovaPrep LLC, Drexel, MO, US) and eluted 3 times with 250 µL TRIS/Tween buffer. A 750 µL aliquot of DNA/RNA Shield was immediately added to each sample and stored at -80 °C for RNA processing.

Chemical analysis

Chemical analysis was carried out on the T0 and spent ersatz WPA media at the four different time points (T1, T2, T3, T4) for SuG, R and S treatments (39 samples total) using Ion Chromatography (IC), Inductively Coupled Plasma Optical Emission spectroscopy (ICP-OES), and Total organic carbon (TOC) technique. The IC (Dionex^{TM} ICS-6000, Thermo Scientific) was used to measure the concentrations of anions (sulfate, nitrate, phosphate) and that of cations (Ammonium and Magnesium). The IC anion analysis was done using a 6-point calibration,)0.1, 0.2, 0.5, 0.75, 1.0, and 2.0 ppm), for the anions and the IC cation analysis was done using an 8-point calibration, (0.1, 0.2, 0.5, 0.75, 1.0, 2.0, 5.0, and 10.0 ppm). The ICP-OES analysis was conducted using a Thermo Fisher Scientific iCAP 7600 ICP-OES with sample introduction via Teledyne CETAC Technologies ASX-560 autosampler. Pump speed was set to 50 rpm with the nebulizer at 0.85 L/min and auxiliary gas flow at 0.5 L/min. Coolant gas flow was 12 L/min, and RF power was 1250 W. Exposure to UV and visible light was 30 and 5 seconds respectively. For our analysis, the instrument was calibrated in the 0 to 1 ppm range, for the elements: phosphorus, magnesium, and silicon. TOC analysis was conducted using a Fusion TOC analyzer (Teledyne Instruments). The system was calibrated using an 8-point calibration (0, 0.2, 0.5, 1, 2.5, 5, 8 and 10 ppm); and samples were prepared with a 10X dilution to fit into the calibration range.

CFU/mL Plate Count

Serial dilutions in 0.9 % sterile saline were prepared to $10^8$and 100 µL were plated in duplicate onto TSA. Plates were incubated at 27 °C overnight and counts were recorded for each plate the next day to determine CFU/mL.

Crystal Violet Stain Protocol

A Crystal Violet Stain method (Wang et al. 2016) was used to evaluate the amount of biofilm attached to the HARV interior surfaces during each experiment. Briefly, sterile DiH_2O was used to rinse out non-biofilm debris from the overnight dried HARVs using a 50 mL disposable pipette. Then 50 mL of 0.1% crystal violet stain solution was added to the HARV and incubated at room temperature for 15 minutes. The crystal violet stain was removed and the HARV was rinsed with sterile DI water to remove any remaining stain and the HARVs were allowed to dry for 24 hours. After 24 hours, 2 mL of 100% dimethyl sulfoxide (DMSO) was applied to the HARV to solubilize any remaining crystal violet. The DMSO was swirled in the HARV to ensure maximum crystal violet solubilization then drained into a cuvette. The crystal violet-DMSO absorbance was read at OD600.

RNA extraction & Library Prep

Total RNA was isolated from each of the 39 samples using the Direct-zol RNA Miniprep Plus Kit (Zymo Research, Irvine, CA, US) with TriReagent as per manufacturer's protocol with the following modifications: each sample was processed in duplicate starting with 500 µL each of the sample and TriReagent in a 2 mL tube with 3 mm sterile glass beads. The tubes were processed with a Bead Ruptor Elite Homogenizer at 6.3 m/s for 30 s and repeated 3 times with a dwell time of 15 s between each round (OMNI International, Kennesaw, GA, US). Like samples were pooled into a 15 mL centrifuge tube (Falcon) tube and an equal volume (2 mL) of 100% ethanol was

added and the samples were mixed thoroughly. The samples were applied to the Zymo-Spin columns and centrifuged at 10k x g for 30 s. Repeated applications were made until all the sample was processed. The RNA prewash was completed per the protocol however, the RNA wash was completed in a two-step process to remove any remaining TriReagent which influenced the total RNA quality recovered. Briefly, the first wash was completed with 700 µL of wash buffer and centrifuged at 10k x g for 30 s while a second wash of 350 µL was completed with a 1 min centrifugation step to remove any residual ethanol. Finally, the total RNA was eluted in 50 µL of DNase/RNase free water. Total RNA was quantified with QUBIT RNA HS (high sensitivity) assay and Nanodrop was used to determine quality. Total RNA was processed for ribosomal RNA (rRNA) removal using Illumina Ribo-Zero Plus rRNA Depletion Kit according to manufacturer's protocol (Illumina, Inc., San Diego, CA, US). Following ribodepletion, samples were processed using the TruSeq Stranded Total RNA library preparation kit (Illumina Inc. San Diego, CA, US)) generating individual cDNA libraries with unique dual indexes via IDT for Illumina TruSeq RNA UD Indexes with modifications. In the "Fragment and Denature RNA" step of the library preparation protocol, EPH/EPH3 (Elute, Prime, Fragment High Mix) buffer was replaced with EPF (Elute, Prime, Fragment) buffer from TruSeq RNA Sample Prep Kit-V2 (Illumina Catalog No. 15027387). The "Denature-RNA" PCR program was modified to match the EPF buffer such that the second step was changed to 94 °C for 8 min from 94 °C for 2 min specific for EPH/EPH3. The 39 individual libraries were quantified using Qubit RNA HS/BR kits (ThermoFisher, Invitrogen, Grand Island, NY, US) and diluted to equimolar concentrations for pooling. Individual and pooled libraries were assessed for quality and quantity using the 2100 Bioanalyzer instrument (Agilent, Santa Clara, CA, US) with RNA 6000 Nano kit. Libraries were sequenced on the Illumina the NextSeq 1000 instrument in a 150 X 2 paired-end mode.

RNAseq Analysis

The adapter trimming for the raw reads of the 39 samples by Adapter Removal (v 2. 1.7) was completed on the Illumina MiSeq instrument. FASTQ files were generated through Illumina BaseSpace (cloud-based run monitoring and data analysis) platform. Raw FASTQ files were analyzed using the SAMSA2 pipeline (Westreich et al. 2018). Paired-end files were merged using PEAR v0.9.10 (Zhang et al. 2014) followed by removal of low-quality sequences and/or adaptor contamination using Trimmomatic v0.36 with a quality score of -phred33, SLIDINGWINDOW:4:15 and MINLEN:70 (Bolger, Lohse, and Usadel 2014). SortMeRNA v2.1 was used in the next step to remove any lingering ribosomal RNA after the ribodepletion step during the library prep using the SILVA bacterial 16S (%ID 90) database (Kopylova, Noé, and Touzet 2012). Paired end reads were mapped to the reference genome of *Burkholderia contaminans* strain B17-01563-1 (RefSeq assembly: GCF_022533485.1) using BWA-MEM (v0.7.17). Mapped read pairs were counted for each gene using featureCounts (v1.6.1). This count table was used to construct a dataset in DeSeq2 which prefiltered genes with greater than 10 reads and used the median of ratios method to normalize for sequencing depth and RNA composition. DESeq2 v3.7 was used for statistical analysis of differentially expressed features/transcripts (Love, Huber, and Anders 2014) between all pair-wise comparisons of experimental groups to determine a $\log_2$Fold Change ($\log_2$FC) value.

Data visualization

CFU/ml and biofilm measurements were graphed and the biofilm values were compared using a one-way ANOVA with Tukey's multiple comparison test in GraphPad Prism version 8.0.0 for Windows, GraphPad Software, San Diego, California USA, www.graphpad.com. A principal component analysis (PCA) was carried out on the average value of biological triplicate measurements of nutrient data and log_2FC values and visualized using the 'factoextra' package in R-studio. Volcano plots of log_2FC values were constructed using the 'ggplot2' package. A Venn diagram used to illustrate differentially expressed genes (DEGs, log_2FC of ±2, and a p-value of less than 0.05) and the overlap was constructed using the Venny (2.1.0) GUI. Clustered heatmaps of DEGs (log_2FC of ±2, and a p-value of less than 0.05 in at least one treatment) were constructed with a distance metric of the Pearson correlation and a complete linkage clustering method using the "pheatmap" (v1.0.12) R package.

Results

Monoculture of B. contaminans in ersatz

Burkholderia. contaminans is the second most cultured bacteria from the International Space Station (ISS) water processor assembly (WPA)(O'Rourke et al. 2020). The bacterium was grown as a monoculture in a WPA ersatz formula, which simulates the chemical and organic makeup of the ISS WPA water. The bacteria in WPA ersatz were subjected to three treatments: 1. simulated microgravity (SµG) with vertical rotation, 2. a horizontally rotating (R) control 1G gravity control, and 3. a stationary or static (S) 1G gravity control. Each treatment was conducted in biological triplicate over a time course of four samples which spanned a 50-hour growth curve of the culture. Colony forming units per milliliter (CFU/mL) of bacteria were recorded for each timepoint (Figure 1) and a biofilm assessment using crystal violet was also made (Figure 2). CFU/mL counts show the SµG and R treatments to be greater than the S counts over all time points with each treatment reaching the same final cell counts at T=4 at 50 hours. Biofilm formation was significantly different at timepoint 2, with SµG treatment showing the greatest biofilm formation followed by the R control and then the S treatment.

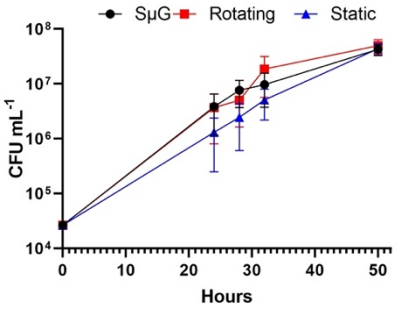

Figure 1: Average CFU/mL for the biological triplicate experiments conducted over three separate days. Error bars represent standard error of the mean.

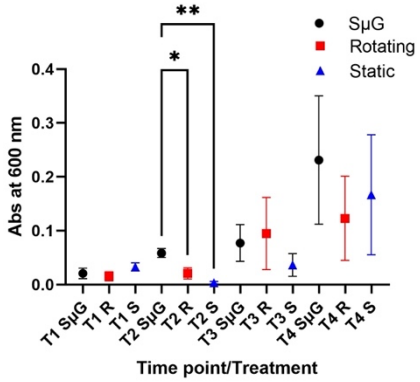

*Figure 2: The symbols represent the average absorbance of crystal violet stain which correlates to amount of biofilm formed in the SuG, rotating and static treatments. Error bars represent one standard deviation of uncertainty. *P=.0313, **P=.0057.*

Ersatz nutrient analysis

The WPA ersatz used to culture the *B. contaminans* bacteria in the HARVS was sampled at time zero (T=0) and at four subsequent timepoints (T1; 24hrs, T2; 28hrs, T3; 32hrs, T4; 50hrs) for each biological triplicate. An ersatz WPA water analysis was conducted and reported on parts per million (ppm) values for the following elements: PO_4^{3-}, Mg, NH_4^+, TOC (Total Organic Carbon), Ca, K, Mg, Si, and SO_4^{2-}

(Supplemental Table 2). The corresponding part per million (ppm) nutrient values for each of the timepoints from each biological replicate were averaged. The collective dataset was subjected to a PCA. The analysis was preformed using all treatments: 1. simulated microgravity (SuG) with vertical rotation, 2. a horizontally rotating (R) control 1G gravity control, 3. a static (S) 1G gravity control showing a clear clustering of S timepoint away from the SuG and R treatments and stratified by timepoint. Figure 3, left panel, illustrates PC1 (Dim 1) explaining 48.1% and PC2 (Dim 2) explaining 32.1% of the variance among samples. In Figure 3, right panel, nutrients are depicted as vectors and their length and direction illustrates their contribution to the stratification of variance and correlation to the sample. For example, in Figure 3, the samples stratify over timepoints according to their correlation with phosphate, magnesium, ammonia, total organic carbon (TOC), potassium, silicon, and sulfate content in the ersatz media. The early and late timepoints of each treatment stratify according to the remaining residual essential nutrients while the later timepoints stratify treatments according to the amount of sulfur, potassium, and silicon available in solution. These results illustrate the uptake of essential nutrients (C, N, P, Mg) and TOC in all treatments and that these nutrients are taken up most quickly in the simulated microgravity treatment. The results further suggest that the R and SuG treatments at the later timepoints are scavenging carbon from the organosilicon substrates (decamethylcyclopentasiloxane, dodecamethylcyclohexasiloxane, octamethylcyclotetrasiloxane, dimethoxydimethylsilane, hexamethylcyclotrisiloxane) of the ersatz media to meet metabolic needs, thus freeing up silicon in solution. This is likely also true for sulfate as it is freed from dimethyl sulfone and potassium as it is free up from potassium phosphate as phosphate is scavenged from solution.

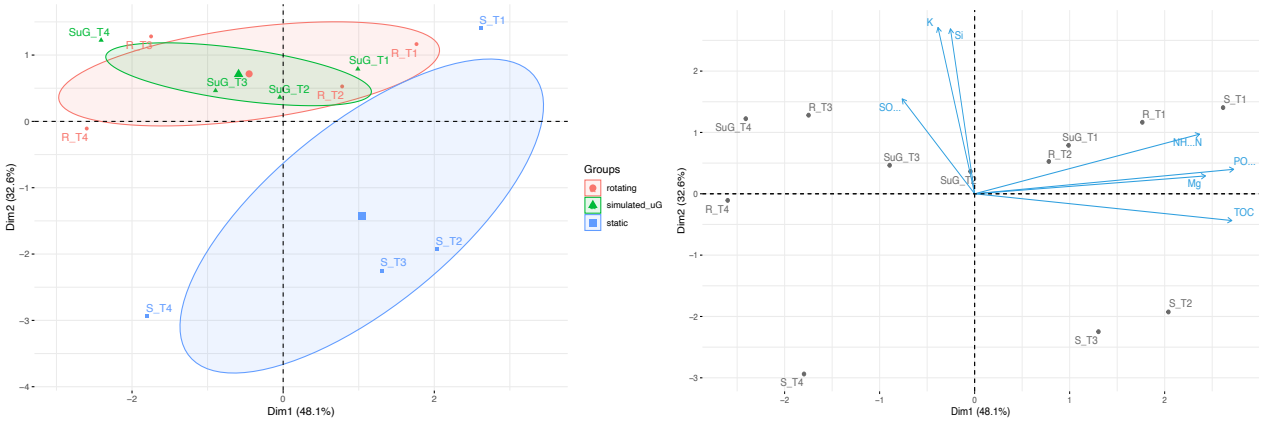

Figure 3: (left panel) Principal Component Analysis of Ersatz Water Nutrient averages per time point per biological replicate for the simulated microgravity (SuG), rotating (R) gravity and static (S) gravity control. (right panel) biplot overlaying nutrient vectors and PCA plot of averaged samples.

Bacterial transcriptomic analysis

The differential gene expression (DGE) for each treatment of SµG, R, and S was determined at each timepoint (T1, T2, T3, and T4) as compared to T0 by generating the $\log_2$ fold change ($\log_2$FC) of the normalized treatment timepoint counts divided by the normalized timepoint 0 counts (Supplemental Table 3). The expression values for the 7733 genes (of the 7768 annotated genes) of treatments SuG, R and S were subject to a PCA (Figure 4). In this analysis the principal

component 1 (PC1 or Dim 1) describes 39.4% of the variance among samples and the PC2 (Dim 2) explains 14.4% of the variation among samples. Overall, the SµG, R and S timepoints show a separate but similar stratification pattern as highlighted by the large ellipses colored according to treatment group with a central solid circle or triangle. Like the timepoint shift in the chemical analysis, SµG timepoint 1 clusters more closely with R timepoint 2 and SuG timepoint 2 clusters closer to the SµG and R timepoint 3. Here, in all treatments, timepoint 4 clusters further apart from the exponential phase timepoints (T1, T2, T3). In a further analysis of the treatment timepoints as compared to T=0, each illustrated the hallmarks for the respective growth phase exhibiting RNA polymerase, ribosomal transporter, and flagellar response activity (Supplemental Table 3).

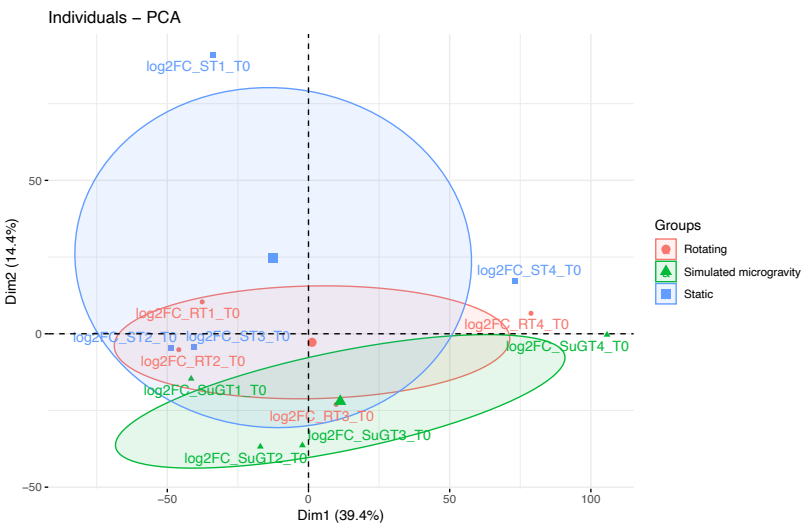

Figure 4: log₂ fold change (log₂FC) of the each timepoint from each treatment, SuG, R, S as compared to T=0.

To look further at the differentially expressed genes (DEGs) for each of the SµG treatment timepoints as compared to the respective R and S control timepoints, the log_2FC was determined from a ratio of the normalized SµG timepoint counts divided by the normalized control timepoint counts (Supplemental Table 4). The results were visualized for each timepoint as volcano plots (Figure 5). 4-fold (log_2FC of 2) down regulated DEGs with p-values less than 0.05 are denoted in blue, 4-fold (log_2FC of 2) up regulated DEGs with p-values less than 0.05 are denoted in red. All other DEGs that do not pass these filters are in black. In summary, the SuG to R control comparison at timepoint 1 has 60 DEGs with maximum log_2FCs of +4.21 and -5.40, timepoint 2 has 106 DEGs with maximum log_2FCs of +4.96 and -5.37, timepoint 3 has 45 DEGs with maximum log_2FCs of +3.31 and -4.46, and timepoint 4 has the most at 143 DEGs with maximum log_2FCs of +7.46 and -3.92 (Figure 5, Supplemental Table 4). The SuG to S control comparison at timepoint 1 has 117 differentially expressed genes (DEGs) with maximum log_2FCs of +3.85 and -5.19, timepoint 2 has 102 DEGs with maximum log_2FCs of +7.06 and -5.22, timepoint 3 has 170 DEGs with maximum log_2FCs of +9.24 and -5.00, and timepoint 4 has the most at 180 DEGs with maximum log_2FCs of +6.58 and -3.65 (Figure 5, Supplemental Table 4). The number of DEGs are similar at each timepoint for the comparison of SuG to control treatments, either R or S, but the maximum and minimum log_2FC are overall larger for the SuG to S comparison as expected from the Figure 4 PCA which clusters the SuG and R timepoints closer to together according to DGE profiles.

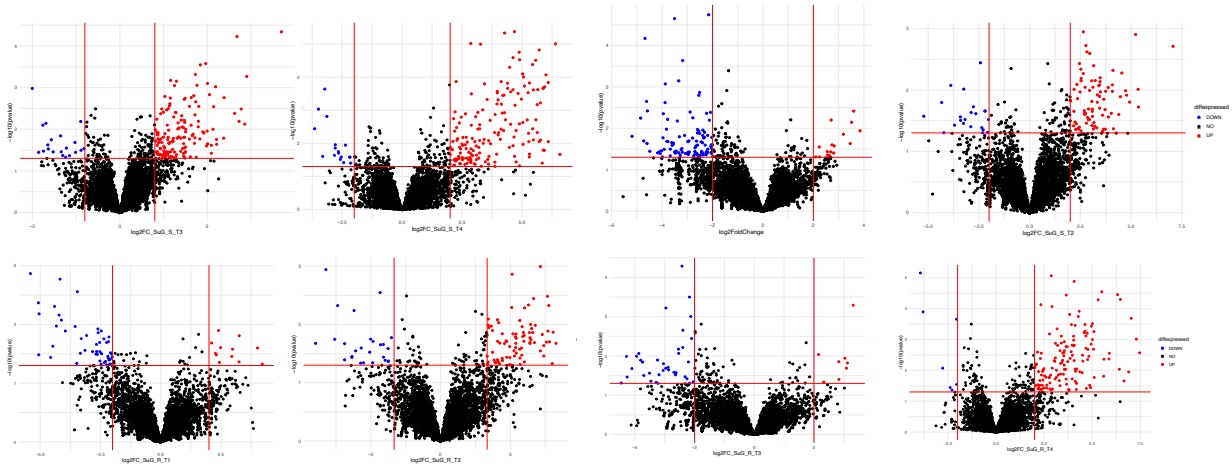

Figure 5: (top panel) Volcano plots for log_2FC values comparing SuG expression to that of the R control. (bottom panel) Volcano plots for log_2FC values comparing simulated SuG expression to that of the S control.

Robust response

With supporting evidence from the spent ersatz media assessment above which provided insight that essential nutrients (C, N, P, Mg) were taken up in all treatments but at a faster rate in the SuG treatment, it is possible to use the transcriptomics analyses to understand how this reduction in nutrients over time affects the cellular response of the SuG treatment as compared to the R and S controls. The 577 DEGs with a greater than 4-fold (log_2FC of 2) up or down regulation and a p-value less than 0.05 in the uG treatment as compared to the R and S control are displayed in Supplemental Table 4 and as a Venn diagram in Figure 6. Among these, 183 are differentially expressed in at least one of the SuG-treatment-to-R and -S controls timepoint comparisons (Figure 6, Supplemental Table 4). We have termed this the 'robust' response. The pattern of DGE for the 183 genes is similar regardless of control and hierarchical clustering shows the

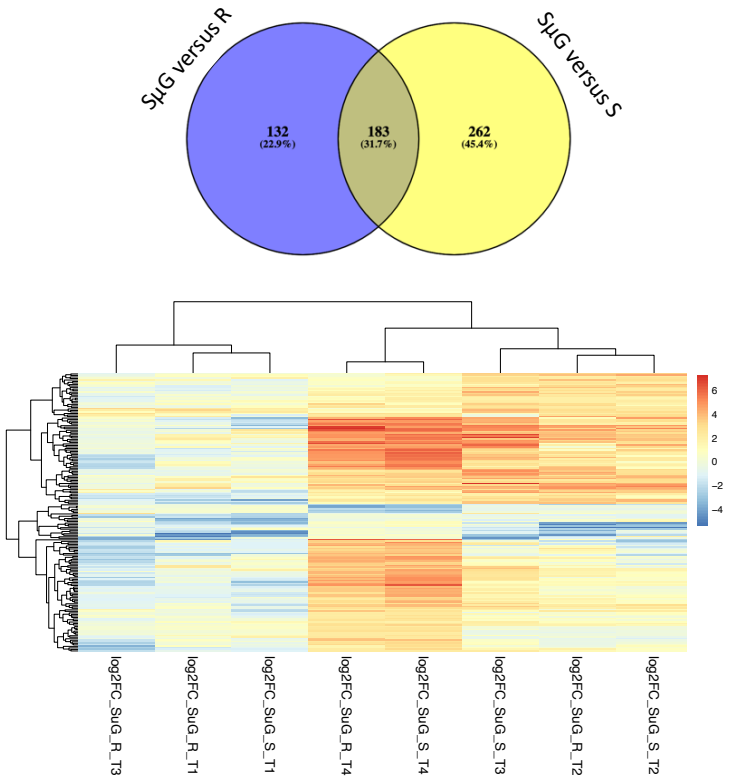

Figure 6. Venn diagram of 577 DEGs with a greater than 4-fold (log_2FC of 2) up or down regulation and a p-value less than 0.05 in the SuG treatment as compared to the R (SuG_R) and S control (SuG_S). Heatmap of log_2FC values and hierarchical clustering for the 183 robust response genes (red shows up-regulated genes and blue shows down-regulated genes) and four timepoints (T#) per the SuG treatment to R (SuG_R) and S controls (SuG_S).

clustering of timepoints T1, T2, T4 except for the T3 comparison for SuG to R showing a greater down regulation of genes as compared to the up regulation of genes exhibited for the SuG to S comparison.

Further evaluation of the 183 gene products within the robust response illustrates that the SuG treatment at timepoint 1 shows a common down regulation when compared to the R and S control timepoint 1 in poly aromatic hydrocarbon breakdown and ABC transporter substrate-binding proteins with an up-regulation in glutamine--fructose-6-phosphate transaminase (isomerizing) using glutamine as a nitrogen source. At timepoint 2, the SuG condition transporter activity is up regulated in relation to both the R and S controls (SulP family inorganic anion transporter, efflux RND transporter periplasmic adaptor subunit, ABC transporter permease), suggesting that the reduced nutrient environment of the SuG culture is starting to be detectable in the transcriptomic response of the cells. For example, the SulP family inorganic anion transporter may be shuttling sulfate to the extracellular environment in exchange for extracellular formate, oxalate, chloride, or bicarbonate as needed for metabolism and from what is available in solution. In timepoint 3, an increase in c-type cytochrome responsible for electron transport in bacterial metabolism is observed as alterative substrates are sourced from solution. Finally, in timepoint 4, signatures of a starvation response are displayed in the upregulation of substrate binding proteins, alcohol dehydrogenases, universal stress proteins, and a toxin of the toxin-antitoxin system. Additionally, an increase in virulence attributes is observed through the upregulation of lectins for host cell binding and type II secretion system proteins (GspF, GspG, GspH), as well as efflux RND transporter elements associated with antibiotic resistance. A predisposition to enhanced biofilm formation is also suggested by the upregulation of polysaccharide biosynthesis and of the enzyme diguanylate cyclase which catalyzes the formation of the bacterial second messenger, c-di-GMP, known to have a role in controlling cellular secretion, cell adhesion and motility leading to biofilm formation and increased cytotoxicity.

Control specific response

Of the 577 DEGs and in addition to the 183 DEGs of the robust response, 132 DEGs were exclusively differentially expressed between the SuG treatment and the R control (Figure 6). At timepoint 1, a down regulation of metabolism, substrate transport, ATP binding and sigma factor activity is illustrated with an up regulation in transcriptomic regulation and oxidoreductase activity. At timepoint 2, the receptors of the iron transporter TonB along with other cell surface transporters are down regulated, whereas, capsular biosynthesis proteins, and ATP binding proteins are upregulated. At timepoint 3, flagellar biosynthesis genes (FlhG,FliD,FlgE,MotA) as well as the antitoxin of the PhD/YefM type II toxin-antitoxin system are downregulated and an up regulation in urea transport and breakdown (ureG and ureA enzymes) is exhibited, suggesting that available urea in the WPA ersatz is being broken down to procure a source of nitrogen. Timepoint 4 had the greatest number of DEGs in the shared robust response but presents nothing notably new in the R control specific response comparison.

Furthermore, 262 DEGs were exclusively differentially expressed between the SuG treatment and the S control. Timepoint 1 similarly illustrates a downregulation in the biological functions of transporter activity, ATP hydrolysis activity, sigma factor activity, and metabolic function and an up regulation in transferase activity. Timepoint 2 saw a down regulation in phosphorelay signal transduction system and choline transport but an up regulation in a toxin of the VapC toxin-antitoxin system II component, flagellar motor switch protein (FliM), and Flp pillus assembly (tadA), suggesting dormancy and surface adhesion mechanism are enhanced under SuG as compared to S control. Timepoint 3 saw a down regulation of transmembrane transport (GO:0055085) and an up regulation in sugar transport and the antitoxin of the of the VapB toxin-antitoxin system II component and type VI secretion system effector, further suggesting dormancy and a decrease in the delivery of protein products to neighboring cells. Timepoint 4 has a downregulation in substrate and amino acid transport and an upregulation in type II secretion system pseudophillin (GspK), phospholipase C activity, and glycosyltransferase activity further suggesting a relative increase in virulence and biofilm formation.

Discussion

Prior spaceflight and LSMMG experimentation which controlled for the phosphate concentrations added to media suggest that nutrient limitation, specifically in the form of phosphate, plays a role in the increased virulence, resistance and cell density outcomes for bacterial cultures exposed to these low-shear environments (Kim et al. 2013; Rosenzweig et al. 2010; Pyle et al. 1999). Given this observation, we aimed to investigate how nutrient reduction over time could be contributing to biofilm formation in the ISS WPA. To evaluate the role of nutrient limitation we conducted a surveillance of the inorganic nutrients and total organic carbon (TOC) and the corresponding transcriptomic profiles of a *B. contaminans* culture in WPA ersatz media over time under a LSMMG simulated microgravity (SuG) treatment and a rotating (R) and static (S) control subject to ambient gravity conditions.

Given that each culture began with the same available nutrients at T=0, our nutrient analysis illustrates that by the first 24-hour timepoint (T=1) at mid exponential phase, the simulated microgravity condition had consumed the essential nutrients defined as C, N, P, Mg and TOC of the WPA ersatz formula more rapidly than either the R or S controls. When evaluating the transcriptomic response of the SuG condition to that of the R and S controls in our robust comparison, the 24-hour culture did not yet appear to show the signatures of nutrient stress. However, starting at the 28-hour timepoint (T=2), stress signals began to steadily increase, leading up to signatures of biofilm, adhesion, virulence, and dormancy mechanisms that were in effect by stationary phase at 50 hours (T=4). This is consistent with the biofilm formation increase at T2 (crystal violet data), as well as the growth decrease between T2 and T3 for simulated microgravity culture (when comparing CFU at T3 and T2).

These observations, which correlate an enhanced predisposition for biofilm formation to a rapid nutrient uptake and the subsequent depletion of nutrients available in solution for simulated microgravity as compared to the rotating and static gravity-subjected controls, have greater implications for how WPA system dormancy contributes to biofilm formation in the microgravity environment of the ISS versus in an Earth-based system. When our analysis is cross checked with

the results from the prior microarray analysis of *P. aeruginosa* PAO1 grown in rich media under LSMMG and compared with a horizontally rotating ambient gravity control at 24 hours (Crabbé et al. 2010), we similarly observe genes encoding chaperones, citric acid cycle enzymes, ATP synthases, and cytochromes to be differentially expressed throughout the timepoints. We do not see the upregulation of the alternative sigma factor AlgU (RpoE-like, analogue to sigma factor-24) reported to be involved in regulating transcripts encoding stress-related proteins, instead we see a down-regulation of sigma factor-24 at 24 hours. When contextualized to the Space Shuttle 6-day endpoint experiment using *B. cepacia* isolated from the Shuttle water system cultured in the low nutrient setting of sterile water, which advanced to full biofilm formation, our 2-day study provides evidence that nutrient starvation is a factor which predisposes *Burkholderia* to biofilm formation (Pyle et al. 1999).

Taken together, our results suggest that if the ISS system is dormant without fresh essential nutrient supply, microbes, which include and extend beyond *B. contaminans*, can begin to adhere to surfaces as biofilms within 24 hours. The extent of the formation will depend on the starting concentration of bacteria, available nutrients, and the duration of dormancy. Currently, ISS WPA maintenance utilizes WPA tank cycling to avoid prolonged dormancy and minimize biofilm accumulation in the tank and downstream component clogging (Weir et al. 2012). Biofilm formation can be further prevented by methods such as maintaining a minimal flow through the system, in combination with other management approaches to employ antimicrobial methods such as surface coatings with inhospitable textures, application of chemical groups or hydrophobic properties.

Acknowledgements
We would like to acknowledge Chelsea McCool and Alexander Johnson of the Marshall Space Flight Center, Jacobs Space Exploration Group, for providing the WPA ersatz mixture for this work.

Funding source
This work was supported by a National Atmospheric and Space Administration, Kennedy Space Center, 2021 Center Innovation Fund.

Reference
Albrecht-Buehler, G. 1991. “Possible Mechanisms of Indirect Gravity Sensing by Cells.” *ASGSB Bulletin: Publication of the American Society for Gravitational and Space Biology* 4 (2): 25–34.

Benoit, Michael R., and David M. Klaus. 2007. “Microgravity, Bacteria, and the Influence of Motility.” *Advances in Space Research* 39 (7): 1225–32. https://doi.org/10.1016/j.asr.2006.10.009.

Bolger, Anthony M., Marc Lohse, and Bjoern Usadel. 2014. “Trimmomatic: A Flexible Trimmer for Illumina Sequence Data.” *Bioinformatics (Oxford, England)* 30 (15): 2114–20. https://doi.org/10.1093/bioinformatics/btu170.

Crabbé, Aurélie, Benny Pycke, Rob Van Houdt, Pieter Monsieurs, Cheryl Nickerson, Natalie Leys, and Pierre Cornelis. 2010. “Response of Pseudomonas Aeruginosa PAO1 to Low Shear

Modelled Microgravity Involves AlgU Regulation." *Environmental Microbiology* 12 (6): 1545–64. https://doi.org/10.1111/j.1462-2920.2010.02184.x.

Diaz, Angie, Wenyan Li, Tesia Irwin, Aubrie O'Rourke, Luz Calle, Mary Hummerick, Christina Khodadad, Jonathan Gleeson, and Michael Callahan. 2022. "Investigation into Simulated Microgravity Techniques Used to Study Biofilm Growth," July. https://ttu-ir.tdl.org/handle/2346/89753.

Diaz, Angie M, Wenyan Li, Tesia D Irwin, Luz M Calle, and Michael R Callahan. n.d. "Investigation of Biofilm Formation and Control for Spacecraft –An Early Literature Review," 17.

Kim, Wooseong, Farah K. Tengra, Zachary Young, Jasmine Shong, Nicholas Marchand, Hon Kit Chan, Ravindra C. Pangule, et al. 2013. "Spaceflight Promotes Biofilm Formation by Pseudomonas Aeruginosa." *PloS One* 8 (4): e62437. https://doi.org/10.1371/journal.pone.0062437.

Klaus, David M., Michael R. Benoit, Emily S. Nelson, and Timmothy G. Hammond. 2004. "Extracellular Mass Transport Considerations for Space Flight Research Concerning Suspended and Adherent in Vitro Cell Cultures." *Journal of Gravitational Physiology: A Journal of the International Society for Gravitational Physiology* 11 (1): 17–27.

Kopylova, Evguenia, Laurent Noé, and Hélène Touzet. 2012. "SortMeRNA: Fast and Accurate Filtering of Ribosomal RNAs in Metatranscriptomic Data." *Bioinformatics (Oxford, England)* 28 (24): 3211–17. https://doi.org/10.1093/bioinformatics/bts611.

Love, Michael I., Wolfgang Huber, and Simon Anders. 2014. "Moderated Estimation of Fold Change and Dispersion for RNA-Seq Data with DESeq2." *Genome Biology* 15 (12): 550. https://doi.org/10.1186/s13059-014-0550-8.

Nauman, Eric A., C. Mark Ott, Ed Sander, Don L. Tucker, Duane Pierson, James W. Wilson, and Cheryl A. Nickerson. 2007. "Novel Quantitative Biosystem for Modeling Physiological Fluid Shear Stress on Cells." *Applied and Environmental Microbiology* 73 (3): 699–705. https://doi.org/10.1128/AEM.02428-06.

O'Rourke, Aubrie, Michael D. Lee, William C. Nierman, R. Craig Everroad, and Chris L. Dupont. 2020. "Genomic and Phenotypic Characterization of Burkholderia Isolates from the Potable Water System of the International Space Station." *PLOS ONE* 15 (2): e0227152. https://doi.org/10.1371/journal.pone.0227152.

"Pyle: Biorack on Spacehab. Biological Experiments... - Google Scholar." n.d. Accessed October 26, 2022. https://scholar.google.com/scholar_lookup?title=Biorack+on+Spacehab:+Biological+Experiments+on+Shuttle+to+Mir+Missions+03,+05+and+06&author=B.+H.+Pyle&author=G.+A.+McFeters&author=S.+C.+Broadaway&author=C.+K.+Johnsrud&author=R.+T.+Storga&publication_year=1999&.

Rosenzweig, Jason A., Ohunene Abogunde, Kayama Thomas, Abidat Lawal, Y.-Uyen Nguyen, Ayodotun Sodipe, and Olufisayo Jejelowo. 2010. "Spaceflight and Modeled Microgravity Effects on Microbial Growth and Virulence." *Applied Microbiology and Biotechnology* 85 (4): 885–91. https://doi.org/10.1007/s00253-009-2237-8.

Sharma, Gayatri, and Patrick D. Curtis. 2022. "The Impacts of Microgravity on Bacterial Metabolism." *Life* 12 (6). https://doi.org/10.3390/life12060774.

Velez Justiniano, Yo-Ann, Donald Carter, Elizabeth Sandvik, Phil Stewart, Darla Goeres, Paul Sturman, Wenyan Li, Alexander Johnson, and Iulian Cioanta. 2021. "Biofilm

Management in a Microgravity Water Recovery System," July. https://ttu-ir.tdl.org/handle/2346/87082.

Wang, Haili, Yanfeng Yan, Dan Rong, Jing Wang, Hongduo Wang, Zizhong Liu, Jiaping Wang, Ruifu Yang, and Yanping Han. 2016. "Increased Biofilm Formation Ability in Klebsiella Pneumoniae after Short-Term Exposure to a Simulated Microgravity Environment." *MicrobiologyOpen* 5 (5): 793–801. https://doi.org/10.1002/mbo3.370.

Weir, Natalee, Mark Wilson, Airan Yoets, Thomas Molina, Rebekah Bruce, and Layne Carter. 2012. "Microbiological Characterization of the International Space Station Water Processor Assembly External Filter Assembly S/N 01." In *42nd International Conference on Environmental Systems*. International Conference on Environmental Systems (ICES). American Institute of Aeronautics and Astronautics. https://doi.org/10.2514/6.2012-3595.

Westreich, Samuel T., Michelle L. Treiber, David A. Mills, Ian Korf, and Danielle G. Lemay. 2018. "SAMSA2: A Standalone Metatranscriptome Analysis Pipeline." *BMC Bioinformatics* 19 (1): 175. https://doi.org/10.1186/s12859-018-2189-z.

Zea, Luis, Zeena Nisar, Phil Rubin, Marta Cortesão, Jiaqi Luo, Samantha A. McBride, Ralf Moeller, et al. 2018. "Design of a Spaceflight Biofilm Experiment." *Acta Astronautica* 148 (July): 294–300. https://doi.org/10.1016/j.actaastro.2018.04.039.

Zea, Luis, Nripesh Prasad, Shawn E. Levy, Louis Stodieck, Angela Jones, Shristi Shrestha, and David Klaus. 2016. "A Molecular Genetic Basis Explaining Altered Bacterial Behavior in Space." *PLOS ONE* 11 (11): e0164359. https://doi.org/10.1371/journal.pone.0164359.

Zhang, Jiajie, Kassian Kobert, Tomáš Flouri, and Alexandros Stamatakis. 2014. "PEAR: A Fast and Accurate Illumina Paired-End ReAd MergeR." *Bioinformatics (Oxford, England)* 30 (5): 614–20. https://doi.org/10.1093/bioinformatics/btt593.